



Crystal structure analysis of [5-(4-methoxyphenyl)-2-methyl-2*H*-1,2,3-triazol-4-yl](thiophen-2-yl)-methanone

Subhrajyoti Bhandary,^a Yarabhally R. Girish,^b Katharigatta N. Venugopala^c and Deepak Chopra^{a*}

Received 26 June 2018

Accepted 24 July 2018

Edited by C. Massera, Università di Parma, Italy

Keywords: crystal structure; 1,2,3-triazole; hydrogen bonding; molecular electrostatic potential; MESP; fingerprint plot.

CCDC reference: 1850683

Supporting information: this article has supporting information at journals.iucr.org/e

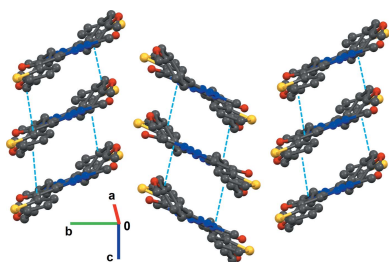
^aCrystallography and Crystal Chemistry Laboratory, Department of Chemistry, Indian Institute of Science Education and Research Bhopal, Bhopal By-pass Road, Bhauri, Bhopal 462 066, Madhya Pradesh, India, ^bDepartment of Organic Chemistry, Indian Institute of Science, Bangalore 560 012, Karnataka, India, and ^cDepartment of Biotechnology and Food Technology, Durban University of Technology, Durban 4001, South Africa. *Correspondence e-mail: dchopra@iiserb.ac.in

The title compound, C₁₅H₁₃N₃O₂S, crystallizes in the monoclinic space group *P*2₁/*n* and its molecular conformation is stabilized *via* intramolecular C—H···O and C—H···N contacts. The supramolecular structure is mainly governed by C—H···N hydrogen-bonded centrosymmetric dimers, C—H···O and C—H···S hydrogen bonds and S···π and π–π stacking interactions which, together, lead to the formation of a layered crystal packing. The intermolecular interactions were further evaluated through the molecular electrostatic potential map and Hirshfeld fingerprint analysis.

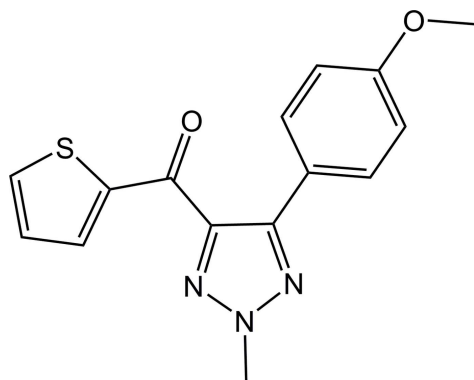
1. Chemical context

Compounds containing the 1,2,3-triazole scaffold are considered to be an important class of five-membered *N*-heterocycles (having two carbon and three nitrogen atoms) because of their unique structural and chemical properties (Kolb & Sharpless, 2003; Freitas *et al.*, 2014). In the last few decades, significant attention has been paid to this kind of structural units owing to their versatile applications in the fields of materials science and medicinal chemistry (Zhou & Wang, 2012; Venugopala *et al.*, 2016). In addition, 1,2,3-triazoles have also been found to be quite relevant in objective-oriented synthesis (Billing & Nilsson, 2005), bioconjugation (Speers *et al.*, 2003) and combinatorial chemistry (Löber *et al.*, 2003). The geometrical shapes and interaction functions of natural heterocycles and amides can be very similar to those of 1,2,3-triazoles (Thibault *et al.*, 2006).

In general, the 1,2,3-triazole nucleus is the most fundamental heterocyclic component found in various pharmacologically active agents (Agalave *et al.*, 2011). In particular, potential pharmaceuticals based on the 1,2,3-triazole ring include anti-HIV (Giffin *et al.*, 2008), anticancer (Singh *et al.*, 2012), anti-tubercular (Patpi *et al.*, 2012), antimicrobial (Demaray *et al.*, 2008) and antifungal (Lass-Floerl *et al.*, 2011) agents. This is due to the fact that the 1,2,3-triazole structural unit is stable against metabolic degradation as well as oxidation and reduction in acidic and basic conditions (Ferreira *et al.*, 2010). Importantly, this special class of structural unit is capable of forming hydrogen-bonding interactions (the N atom acts as an acceptor) as well as π–π stacking and other intermolecular interactions with biological targets to improve



their solubility (Lauria *et al.*, 2014). Hence, it is of extreme importance to explore and understand the supramolecular structure of compounds in which the structural motif is based on 1,2,3-triazole. Keeping in mind the above-mentioned features, we report here the crystal structure and packing analysis of the title compound [5-(4-methoxyphenyl)-2-methyl-2*H*-1,2,3-triazol-4-yl](thiophen-2-yl)methanone (**1**).



2. Structural commentary

The single-crystal X-ray diffraction study shows that compound **1** crystallizes in the monoclinic space group $P2_1/n$ with one molecule ($Z' = 1$) in the asymmetric unit (Fig. 1). In the molecular structure, the *N*-methylated triazol ring is substituted at the two carbon atoms C7 and C8 by a *para*-methoxy phenyl and a methanone-thienyl ring, respectively, resulting in four conformationally flexible parts in the molecule around the C8–C9, C9–C10, C1–C7 and C4–O1 single bonds (see Fig. 1). The conformation of the molecule in the crystal is stabilized *via* intramolecular C2–H2···O2 [C2···O2 = 2.961 (2) Å] and C11–H11···N1 [C11···N1 = 2.950 (2) Å] contacts (Fig. 1; Table 1). For this reason, the thienyl and triazole rings are nearly coplanar, with an angle of 13.63 (10)° between their mean planes, while the phenyl ring is tilted out from the mean planes of the thienyl and triazole

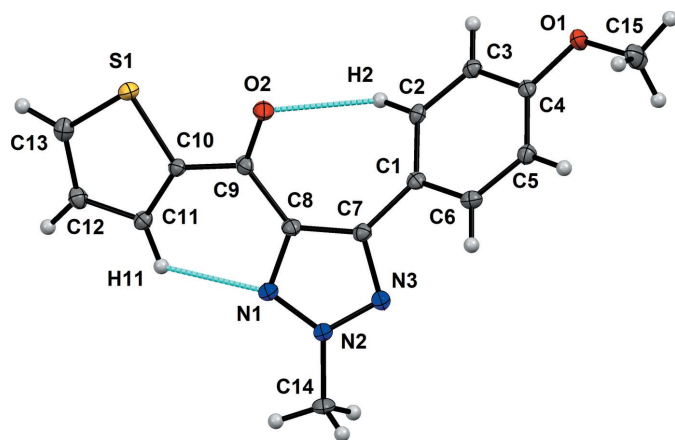


Figure 1

The asymmetric unit of compound **1** highlighting the intramolecular C–H···O and C–H···N contacts. Displacement ellipsoids are drawn at the 50% probability level.

Table 1

Hydrogen-bond geometry (Å, °).

$D-H\cdots A$	$D-H$	$H\cdots A$	$D\cdots A$	$D-H\cdots A$
C11–H11···N1	0.95	2.41	2.950 (2)	116
C2–H2···O2	0.95	2.42	2.961 (2)	113
C3–H3···S1 ⁱ	0.95	2.96	3.810 (2)	149
C15–H15A···O2 ⁱⁱ	0.98	2.98	3.828 (3)	146
C15–H15C···N3 ⁱⁱⁱ	0.98	2.73	3.490 (3)	135
C12–H12···N1 ^{iv}	0.95	2.95	3.768 (2)	145
C13–H13···O2 ^v	0.95	2.38	3.191 (2)	143
C14–H14C···O1 ^{vi}	0.98	2.67	3.230 (2)	117

Symmetry codes: (i) $x + 1, y, z$; (ii) $x + \frac{1}{2}, -y + \frac{1}{2}, z + \frac{1}{2}$; (iii) $-x + 2, -y, -z + 2$; (iv) $-x, -y, -z + 1$; (v) $x - \frac{1}{2}, -y + \frac{1}{2}, z - \frac{1}{2}$; (vi) $-x + \frac{1}{2}, y - \frac{1}{2}, -z + \frac{3}{2}$.

rings by 38.84 (9) and 34.04 (10)°, respectively. It is also important to mention here that the methoxy group attached to C4 is in the same plane as the phenyl ring.

3. Supramolecular features

In the crystal, the molecules form two types of centrosymmetric, weak to very weak C–H···N hydrogen-bonding dimeric motifs (Table 1) involving the methyl hydrogen H15C (sp^3) of the methoxy group with the triazol nitrogen N3 [C15···N3 = 3.490 (3) Å] and the thiophene hydrogen H12 (sp^2) with the triazol nitrogen N1 [C12···N1 = 3.768 (2) Å]. These are extended in an alternate fashion, forming ribbons along the [101] direction (see green and yellow shades in Fig. 2). Two such adjacent hydrogen-bonded ribbons are connected to each other *via* $Csp^2/sp^3-H\cdots O$ and $S\cdots C(\pi)$ [3.492 (2) Å] interactions along the [010] direction, forming a corrugated sheet perpendicular to the (101) plane (Fig. 2 and Table 1). These sheets are further stacked to each other by displaced π – π stacking interactions distances ranging from 3.375 (3) to 3.384 (4) Å through inversion and translational symmetries, and weak C3–H3···S1 [C3···S1 = 3.810 (2) Å] interactions (Table 1), leading to the formation of a layered packing arrangement of molecules (Fig. 3).

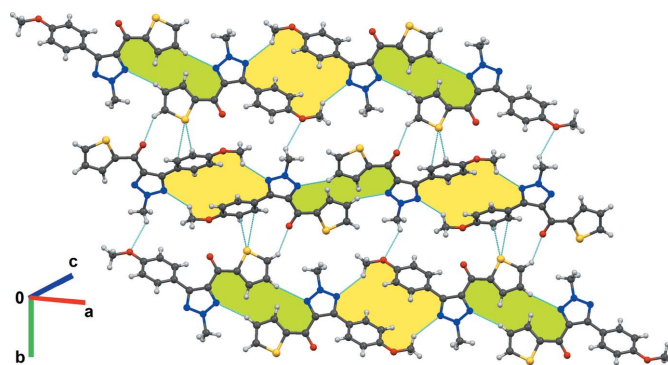


Figure 2

Crystal packing of **1** showing the formation of molecular sheets *via* two types of centrosymmetric C–H···N dimers (shaded in light yellow and green), forming ribbons connected through C–H···O and S···C(π) interactions.

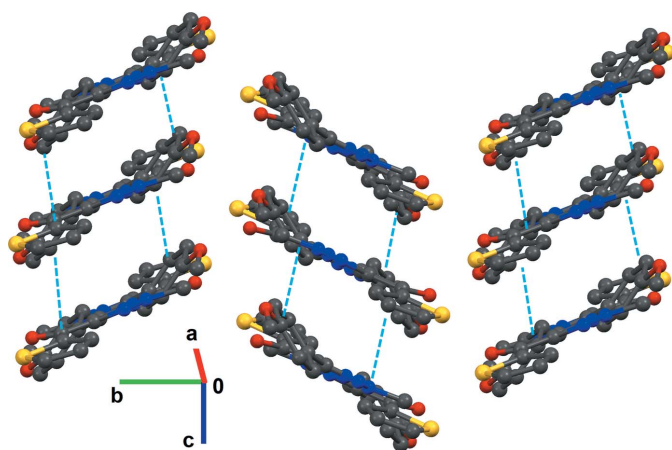


Figure 3
Stacking of hydrogen-bonded molecular sheets *via* π - π interactions (dotted lines) in compound **1**. Hydrogen atoms are omitted for clarity.

4. Analysis of molecular electrostatic potential and Hirshfeld fingerprint plots

A deeper insight into intermolecular interactions can be obtained from molecular electrostatic potential (MESP), and two-dimensional fingerprint plots (McKinnon *et al.*, 2007) mapped on the Hirshfeld surface (Spackman & Jayatilaka, 2009). All the plots were computed using the programme *CrystalExplorer 17.5* (Turner *et al.*, 2017). The MESP plot of compound **1** (Fig. 4) shows that the centres of both the triazole and thiophene five-membered rings have nearly neutral ESP values (0.000 and -0.002 a.u., respectively), while the benzene ring is highly electronegative (-0.028 a.u.) compared to the two heterocyclic rings. This electrostatic complementarity among the rings leads to favourable stacking interactions in the crystal packing as a result of a layered supramolecular architecture. Intermolecular hydrogen-bond donors and acceptors appear as blue (positive ESP) and red (negative ESP) regions, respectively, on the surface (Fig. 4). The two-

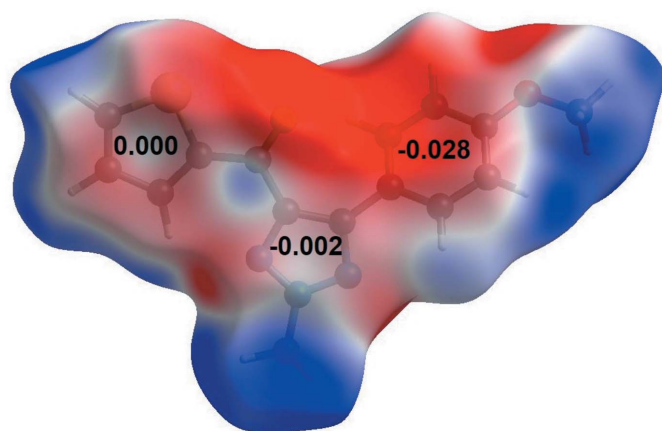


Figure 4
MESP of compound **1** mapped over the Hirshfeld surface with a scale of -0.03 a.u. (red) through 0.00 (white) to $+0.03$ a.u. (blue). The ESP values (in a.u.) for the centre of each ring are given.

dimensional fingerprint plots and the contributions of individual interatomic contacts toward the overall crystal packing are shown in Fig. 5. It is observed that several directional hydrogen-bonding contacts such as $N\cdots H$ (7.7%), $O\cdots H$ (11.0%), $S\cdots H$ (6.3%) along with $C\cdots H$ (18.5%), $H\cdots H$ (41.6%) and other interatomic contacts stabilize the crystal packing of compound **1**.

5. Database survey

A Cambridge Structural Database (Version 5.39, update May 2018; Groom *et al.*, 2016) search for the (2-methyl-2H-1,2,3-triazol-4-yl)(thiophen-2-yl)methanone subunit resulted in one hit (SONFIM; Girish *et al.*, 2014). Like compound **1**, the molecular conformation of SONFIM is also stabilized by intramolecular $C-H\cdots O$ and $C-H\cdots N$ hydrogen bonds. The supramolecular structure of SONFIM is primarily determined by intermolecular $C-H\cdots O$ and $C-H\cdots\pi$ hydrogen bonds, while $C-H\cdots N$ hydrogen bonding plays a secondary role in the overall stabilization of the crystal packing.

6. Synthesis and crystallization

The title compound was synthesized according to the procedure described elsewhere (Girish *et al.*, 2014). Single crystals of the pure compound were grown by slow evaporation of a toluene solution at room temperature (297–301 K).

7. Refinement

Crystal data, data collection and structure refinement details are given in Table 2. Hydrogen atoms were positioned geometrically and refined as riding: $C-H = 0.98$ Å with $U_{iso}(H) = 1.5U_{eq}(C)$ for the methyl group and $C-H = 0.95$ Å with $U_{iso}(H) = 1.2U_{eq}(C)$ for the aromatic C atoms.

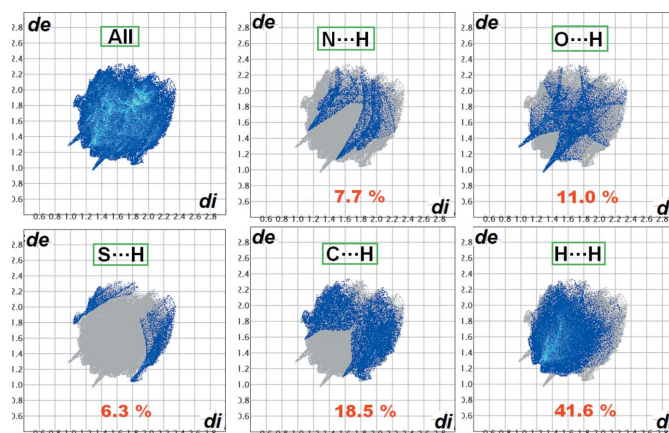


Figure 5
Two-dimensional full fingerprint plots and decomposed fingerprint plots over the Hirshfeld surface for various intermolecular atom-atom contacts in compound **1**. The numbers in red indicate the percentage contributions of each contact.

Table 2

Experimental details.

Crystal data	
Chemical formula	C ₁₅ H ₁₃ N ₃ O ₂ S
<i>M_r</i>	299.34
Crystal system, space group	Monoclinic, <i>P2₁/n</i>
Temperature (K)	100
<i>a</i> , <i>b</i> , <i>c</i> (Å)	8.5851 (10), 16.8986 (19), 9.3455 (11)
β (°)	92.465 (4)
<i>V</i> (Å ³)	1354.6 (3)
<i>Z</i>	4
Radiation type	Mo <i>K</i> α
μ (mm ⁻¹)	0.25
Crystal size (mm)	0.30 × 0.10 × 0.06
Data collection	
Diffractometer	Bruker APEXII D8 Venture CMOS
Absorption correction	Multi-scan (<i>SADABS</i> ; Bruker, 2012)
<i>T_{min}</i> , <i>T_{max}</i>	0.619, 0.746
No. of measured, independent and observed [<i>I</i> > 2 σ (<i>I</i>)] reflections	17149, 3962, 2914
<i>R_{int}</i>	0.065
(<i>sin</i> θ / λ) _{max} (Å ⁻¹)	0.705
Refinement	
<i>R</i> [<i>F</i> ² > 2 σ (<i>F</i> ²)], <i>wR</i> (<i>F</i> ²), <i>S</i>	0.053, 0.114, 1.03
No. of reflections	3962
No. of parameters	192
H-atom treatment	H-atom parameters constrained
$\Delta\rho_{\text{max}}$, $\Delta\rho_{\text{min}}$ (e Å ⁻³)	0.46, -0.53

Computer programs: *APEX2* and *SAINTE* (Bruker, 2012), *SIR2014* (Burla *et al.*, 2015), *SHELXL2018* (Sheldrick, 2015), *Mercury* (Macrae *et al.*, 2006), *WinGX* (Farrugia, 2012) and *PLATON* (Spek, 2009).

Funding information

SB acknowledges IISER Bhopal for a senior research fellowship. DC and SB thank IISER Bhopal for the research facilities and infrastructure. KNV acknowledges the National Research Foundation (96807 and 98884), South Africa, and Durban University of Technology, South Africa, for support and encouragement.

References

- Agalave, S. G., Maujan, S. R. & Pore, V. S. (2011). *Chem. Asian J.* **6**, 2696–2718.
 Billing, J. F. & Nilsson, U. J. (2005). *J. Org. Chem.* **70**, 4847–4850.
 Bruker (2012). *APEX2*, *SAINTE* and *SADABS*. Bruker AXS Inc., Madison, Wisconsin, USA.

- Burla, M. C., Caliandro, R., Carrozzini, B., Cascarano, G. L., Cuocci, C., Giacovazzo, C., Mallamo, M., Mazzone, A. & Polidori, G. (2015). *J. Appl. Cryst.* **48**, 306–309.
 Demaray, J. A., Thuener, J. E., Dawson, M. N. & Sucheck, S. J. (2008). *Bioorg. Med. Chem. Lett.* **18**, 4868–4871.
 Farrugia, L. J. (2012). *J. Appl. Cryst.* **45**, 849–854.
 Ferreira, S. B., Sodero, A. C. R., Cardoso, M. F. C., Lima, E. S., Kaiser, C. R., Silva, F. P. & Ferreira, V. F. (2010). *J. Med. Chem.* **53**, 2364–2375.
 Freitas, L. B. de O., Borgati, T. F., de Freitas, R. P., Ruiz, A. L. T. G., Marchetti, G. M., de Carvalho, J. E., da Cunha, E. F. F., Ramalho, T. C. & Alves, R. B. (2014). *Eur. J. Med. Chem.* **84**, 595–604.
 Giffin, M. J., Heaslet, H., Brik, A., Lin, Y.-C., Cauvi, G., Wong, C.-H., McRee, D. E., Elder, J. H., Stout, C. D. & Torbett, B. E. (2008). *J. Med. Chem.* **51**, 6263–6270.
 Girish, Y. R., Sharath Kumar, K. S., Muddegowda, U., Lokanath, N. K., Rangappa, K. S. & Shashikanth, S. (2014). *RSC Adv.* **4**, 55800–55806.
 Groom, C. R., Bruno, I. J., Lightfoot, M. P. & Ward, S. C. (2016). *Acta Cryst.* **B72**, 171–179.
 Kolb, H. C. & Sharpless, K. B. (2003). *Drug Discovery Today*, **8**, 1128–1137.
 Lass-Floerl, C. (2011). *Drugs*, **71**, 2405–2419.
 Lauria, A., Delisi, R., Mingoia, F., Terenzi, A., Martorana, A., Barone, G. & Almerico, A. M. (2014). *Eur. J. Org. Chem.* **2014**, 3289–3306.
 Löber, S., Rodriguez-Loaiza, P. & Gmeiner, P. (2003). *Org. Lett.* **5**, 1753–1755.
 Macrae, C. F., Edgington, P. R., McCabe, P., Pidcock, E., Shields, G. P., Taylor, R., Towler, M. & van de Streek, J. (2006). *J. Appl. Cryst.* **39**, 453–457.
 McKinnon, J. J., Jayatilaka, D. & Spackman, M. A. (2007). *Chem. Commun.* 3814–3816.
 Patpi, S. R., Pulipati, L., Yogeewari, P., Sriram, D., Jain, N., Sridhar, B., Murthy, R., Anjana Devi, T., Kalivendi, S. V. & Kantevari, S. (2012). *J. Med. Chem.* **55**, 3911–3922.
 Sheldrick, G. M. (2015). *Acta Cryst.* **C71**, 3–8.
 Singh, P., Raj, R., Kumar, V., Mahajan, M. P., Bedi, P. M. S., Kaur, T. & Saxena, A. K. (2012). *Eur. J. Med. Chem.* **47**, 594–600.
 Spackman, M. A. & Jayatilaka, D. (2009). *CrystEngComm*, **11**, 19–32.
 Speers, A. E., Adam, G. C. & Cravatt, B. F. (2003). *J. Am. Chem. Soc.* **125**, 4686–4687.
 Spek, A. L. (2009). *Acta Cryst.* **D65**, 148–155.
 Thibault, R. J., Takizawa, K., Lowenheim, P., Helms, B., Mynar, J. L., Fréchet, J. M. J. & Hawker, C. J. (2006). *J. Am. Chem. Soc.* **128**, 12084–12085.
 Turner, M. J., McKinnon, J. J., Wolff, S. K., Grimwood, D. J., Spackman, P. R., Jayatilaka, D. & Spackman, M. A. (2017). *CrystalExplorer 17.5*. University of Western Australia.
 Venugopala, K. N., Rao, D., Bhandary, S., Pillay, M., Chopra, D., Aldhubiabi, B. E., Attimarad, M., Alwassil, O. I., Harsha, S. & Mlisana, K. (2016). *Drug. Des. Dev. Ther.* **10**, 2681–2690.
 Zhou, C.-H. & Wang, Y. (2012). *Curr. Med. Chem.* **19**, 239–280.

supporting information

Acta Cryst. (2018). E74, 1178-1181 [https://doi.org/10.1107/S2056989018010654]

Crystal structure analysis of [5-(4-methoxyphenyl)-2-methyl-2H-1,2,3-triazol-4-yl](thiophen-2-yl)methanone

Subhrajyoti Bhandary, Yarabhally R. Girish, Katharigatta N. Venugopala and Deepak Chopra

Computing details

Data collection: *APEX2* (Bruker, 2012); cell refinement: *SAINTE* (Bruker, 2012); data reduction: *SAINTE* (Bruker, 2012); program(s) used to solve structure: *SIR2014* (Burla *et al.*, 2015); program(s) used to refine structure: *SHELXL2018* (Sheldrick, 2015); molecular graphics: *Mercury* (Macrae *et al.*, 2006); software used to prepare material for publication: *WinGX* (Farrugia, 2012) and *PLATON* (Spek, 2009).

[5-(4-Methoxyphenyl)-2-methyl-2H-1,2,3-triazol-4-yl](thiophen-2-yl)methanone

Crystal data

C₁₅H₁₃N₃O₂S

M_r = 299.34

Monoclinic, *P2₁/n*

a = 8.5851 (10) Å

b = 16.8986 (19) Å

c = 9.3455 (11) Å

β = 92.465 (4)°

V = 1354.6 (3) Å³

Z = 4

F(000) = 624

D_x = 1.468 Mg m⁻³

Mo *K*α radiation, λ = 0.71073 Å

Cell parameters from 6642 reflections

θ = 2.4–30.0°

μ = 0.25 mm⁻¹

T = 100 K

Plate, yellow

0.30 × 0.10 × 0.06 mm

Data collection

Bruker APEXII D8 Venture CMOS diffractometer

φ and ω scans

Absorption correction: multi-scan (SADABS; Bruker, 2012)

T_{min} = 0.619, *T_{max}* = 0.746

17149 measured reflections

3962 independent reflections

2914 reflections with *I* > 2σ(*I*)

R_{int} = 0.065

θ_{\max} = 30.1°, θ_{\min} = 2.4°

h = -12→11

k = -23→23

l = -10→13

Refinement

Refinement on *F*²

Least-squares matrix: full

R[*F*² > 2σ(*F*²)] = 0.053

wR(*F*²) = 0.114

S = 1.03

3962 reflections

192 parameters

0 restraints

Hydrogen site location: inferred from neighbouring sites

H-atom parameters constrained

$w = 1/[\sigma^2(F_o^2) + (0.037P)^2 + 1.3716P]$

where $P = (F_o^2 + 2F_c^2)/3$

(Δ/σ)_{max} < 0.001

$\Delta\rho_{\max} = 0.46 \text{ e \AA}^{-3}$

$\Delta\rho_{\min} = -0.53 \text{ e \AA}^{-3}$

Special details

Geometry. All esds (except the esd in the dihedral angle between two l.s. planes) are estimated using the full covariance matrix. The cell esds are taken into account individually in the estimation of esds in distances, angles and torsion angles; correlations between esds in cell parameters are only used when they are defined by crystal symmetry. An approximate (isotropic) treatment of cell esds is used for estimating esds involving l.s. planes.

Fractional atomic coordinates and isotropic or equivalent isotropic displacement parameters (\AA^2)

	<i>x</i>	<i>y</i>	<i>z</i>	$U_{\text{iso}}^*/U_{\text{eq}}$
S1	0.22992 (6)	0.20914 (3)	0.39316 (5)	0.01627 (13)
O1	1.18053 (15)	0.18243 (8)	0.81322 (14)	0.0166 (3)
O2	0.48083 (16)	0.18611 (8)	0.60466 (16)	0.0200 (3)
N1	0.35646 (18)	-0.00987 (9)	0.68224 (18)	0.0160 (3)
N3	0.57606 (18)	-0.03357 (10)	0.81538 (18)	0.0158 (3)
N2	0.43569 (18)	-0.05846 (9)	0.76814 (18)	0.0162 (3)
C1	0.7388 (2)	0.08137 (10)	0.7775 (2)	0.0130 (4)
C11	0.1653 (2)	0.06385 (11)	0.4486 (2)	0.0137 (4)
H11	0.167530	0.012226	0.488904	0.016*
C4	1.0365 (2)	0.14778 (10)	0.8101 (2)	0.0130 (4)
C3	0.9476 (2)	0.15862 (11)	0.6832 (2)	0.0132 (4)
H3	0.988464	0.188552	0.607394	0.016*
C7	0.5901 (2)	0.03848 (11)	0.7557 (2)	0.0132 (4)
C5	0.9775 (2)	0.10385 (11)	0.9210 (2)	0.0150 (4)
H5	1.037167	0.096550	1.007982	0.018*
C10	0.2700 (2)	0.12300 (11)	0.4876 (2)	0.0128 (4)
C6	0.8294 (2)	0.07061 (11)	0.9028 (2)	0.0147 (4)
H6	0.789370	0.039832	0.977967	0.018*
C2	0.8005 (2)	0.12602 (11)	0.6675 (2)	0.0131 (4)
H2	0.740456	0.134022	0.580881	0.016*
C8	0.4519 (2)	0.05345 (11)	0.6724 (2)	0.0138 (4)
C9	0.4044 (2)	0.12489 (11)	0.5897 (2)	0.0141 (4)
C15	1.2758 (2)	0.17414 (14)	0.9413 (2)	0.0245 (5)
H15A	1.224395	0.199444	1.020945	0.037*
H15B	1.376982	0.199448	0.928427	0.037*
H15C	1.291563	0.117828	0.962413	0.037*
C12	0.0541 (2)	0.08913 (12)	0.3416 (2)	0.0160 (4)
H12	-0.026154	0.056184	0.301494	0.019*
C13	0.0753 (2)	0.16613 (12)	0.3025 (2)	0.0173 (4)
H13	0.011053	0.192791	0.232674	0.021*
C14	0.3821 (2)	-0.13873 (11)	0.7969 (2)	0.0213 (4)
H14A	0.273221	-0.144368	0.762375	0.032*
H14B	0.390158	-0.148830	0.900188	0.032*
H14C	0.446872	-0.176823	0.747341	0.032*

Atomic displacement parameters (\AA^2)

	U^{11}	U^{22}	U^{33}	U^{12}	U^{13}	U^{23}
S1	0.0164 (2)	0.0123 (2)	0.0201 (3)	-0.00008 (18)	0.00098 (18)	0.00335 (19)

O1	0.0124 (6)	0.0188 (7)	0.0183 (7)	-0.0030 (5)	-0.0029 (5)	0.0017 (6)
O2	0.0164 (7)	0.0107 (6)	0.0325 (8)	-0.0021 (5)	-0.0028 (6)	0.0009 (6)
N1	0.0151 (8)	0.0118 (7)	0.0209 (9)	0.0003 (6)	-0.0009 (7)	0.0019 (7)
N3	0.0124 (8)	0.0154 (8)	0.0195 (8)	-0.0002 (6)	-0.0003 (6)	0.0005 (7)
N2	0.0135 (8)	0.0125 (8)	0.0223 (9)	-0.0006 (6)	-0.0013 (7)	0.0036 (7)
C1	0.0136 (9)	0.0092 (8)	0.0162 (10)	0.0008 (7)	0.0014 (7)	-0.0018 (7)
C11	0.0150 (9)	0.0120 (8)	0.0143 (9)	0.0017 (7)	0.0010 (7)	-0.0010 (7)
C4	0.0123 (8)	0.0094 (8)	0.0173 (9)	0.0006 (7)	0.0001 (7)	-0.0019 (7)
C3	0.0143 (9)	0.0117 (8)	0.0136 (9)	0.0019 (7)	0.0019 (7)	-0.0002 (7)
C7	0.0139 (9)	0.0110 (8)	0.0148 (9)	0.0012 (7)	0.0020 (7)	-0.0002 (7)
C5	0.0143 (9)	0.0150 (9)	0.0154 (9)	0.0009 (7)	-0.0012 (7)	0.0002 (7)
C10	0.0121 (9)	0.0105 (8)	0.0160 (9)	0.0017 (7)	0.0028 (7)	0.0008 (7)
C6	0.0173 (9)	0.0123 (9)	0.0145 (9)	-0.0005 (7)	0.0022 (7)	0.0008 (7)
C2	0.0132 (9)	0.0124 (8)	0.0136 (9)	0.0032 (7)	-0.0004 (7)	-0.0010 (7)
C8	0.0138 (9)	0.0099 (8)	0.0178 (10)	-0.0005 (7)	0.0009 (7)	-0.0010 (7)
C9	0.0115 (9)	0.0116 (8)	0.0193 (10)	0.0012 (7)	0.0028 (7)	-0.0015 (7)
C15	0.0189 (10)	0.0338 (12)	0.0203 (11)	-0.0080 (9)	-0.0066 (8)	0.0034 (9)
C12	0.0144 (9)	0.0170 (9)	0.0164 (10)	-0.0014 (7)	-0.0015 (7)	-0.0028 (8)
C13	0.0160 (9)	0.0204 (10)	0.0156 (10)	0.0025 (7)	0.0000 (7)	-0.0005 (8)
C14	0.0199 (10)	0.0116 (9)	0.0322 (12)	-0.0030 (8)	-0.0010 (9)	0.0070 (8)

Geometric parameters (Å, °)

S1—C13	1.706 (2)	C3—C2	1.380 (3)
S1—C10	1.7292 (19)	C3—H3	0.9500
O1—C4	1.368 (2)	C7—C8	1.413 (3)
O1—C15	1.427 (2)	C5—C6	1.394 (3)
O2—C9	1.230 (2)	C5—H5	0.9500
N1—N2	1.317 (2)	C10—C9	1.466 (3)
N1—C8	1.353 (2)	C6—H6	0.9500
N3—N2	1.334 (2)	C2—H2	0.9500
N3—C7	1.347 (2)	C8—C9	1.481 (3)
N2—C14	1.461 (2)	C15—H15A	0.9800
C1—C6	1.390 (3)	C15—H15B	0.9800
C1—C2	1.398 (3)	C15—H15C	0.9800
C1—C7	1.475 (3)	C12—C13	1.365 (3)
C11—C10	1.383 (3)	C12—H12	0.9500
C11—C12	1.419 (3)	C13—H13	0.9500
C11—H11	0.9500	C14—H14A	0.9800
C4—C5	1.388 (3)	C14—H14B	0.9800
C4—C3	1.394 (3)	C14—H14C	0.9800
C13—S1—C10	91.62 (9)	C1—C6—H6	119.2
C4—O1—C15	117.45 (15)	C5—C6—H6	119.2
N2—N1—C8	103.66 (15)	C3—C2—C1	120.72 (17)
N2—N3—C7	104.09 (15)	C3—C2—H2	119.6
N1—N2—N3	116.16 (15)	C1—C2—H2	119.6
N1—N2—C14	122.16 (16)	N1—C8—C7	108.49 (16)

N3—N2—C14	121.29 (16)	N1—C8—C9	121.73 (16)
C6—C1—C2	118.34 (17)	C7—C8—C9	129.73 (17)
C6—C1—C7	120.11 (17)	O2—C9—C10	119.57 (17)
C2—C1—C7	121.13 (17)	O2—C9—C8	119.53 (17)
C10—C11—C12	112.23 (17)	C10—C9—C8	120.88 (16)
C10—C11—H11	123.9	O1—C15—H15A	109.5
C12—C11—H11	123.9	O1—C15—H15B	109.5
O1—C4—C5	124.87 (17)	H15A—C15—H15B	109.5
O1—C4—C3	115.02 (17)	O1—C15—H15C	109.5
C5—C4—C3	120.10 (17)	H15A—C15—H15C	109.5
C2—C3—C4	120.21 (18)	H15B—C15—H15C	109.5
C2—C3—H3	119.9	C13—C12—C11	112.45 (17)
C4—C3—H3	119.9	C13—C12—H12	123.8
N3—C7—C8	107.60 (16)	C11—C12—H12	123.8
N3—C7—C1	118.64 (16)	C12—C13—S1	112.53 (15)
C8—C7—C1	133.56 (17)	C12—C13—H13	123.7
C4—C5—C6	118.99 (17)	S1—C13—H13	123.7
C4—C5—H5	120.5	N2—C14—H14A	109.5
C6—C5—H5	120.5	N2—C14—H14B	109.5
C11—C10—C9	132.22 (17)	H14A—C14—H14B	109.5
C11—C10—S1	111.18 (14)	N2—C14—H14C	109.5
C9—C10—S1	116.60 (13)	H14A—C14—H14C	109.5
C1—C6—C5	121.63 (18)	H14B—C14—H14C	109.5
C8—N1—N2—N3	-0.6 (2)	C4—C5—C6—C1	-1.0 (3)
C8—N1—N2—C14	-173.55 (18)	C4—C3—C2—C1	-0.4 (3)
C7—N3—N2—N1	0.5 (2)	C6—C1—C2—C3	-0.1 (3)
C7—N3—N2—C14	173.46 (18)	C7—C1—C2—C3	-172.69 (17)
C15—O1—C4—C5	-1.4 (3)	N2—N1—C8—C7	0.5 (2)
C15—O1—C4—C3	179.19 (17)	N2—N1—C8—C9	-177.17 (17)
O1—C4—C3—C2	179.69 (16)	N3—C7—C8—N1	-0.3 (2)
C5—C4—C3—C2	0.2 (3)	C1—C7—C8—N1	174.3 (2)
N2—N3—C7—C8	-0.1 (2)	N3—C7—C8—C9	177.16 (19)
N2—N3—C7—C1	-175.62 (16)	C1—C7—C8—C9	-8.3 (4)
C6—C1—C7—N3	-30.9 (3)	C11—C10—C9—O2	179.7 (2)
C2—C1—C7—N3	141.55 (18)	S1—C10—C9—O2	0.5 (2)
C6—C1—C7—C8	155.0 (2)	C11—C10—C9—C8	1.3 (3)
C2—C1—C7—C8	-32.5 (3)	S1—C10—C9—C8	-177.88 (14)
O1—C4—C5—C6	-178.95 (17)	N1—C8—C9—O2	166.57 (18)
C3—C4—C5—C6	0.4 (3)	C7—C8—C9—O2	-10.5 (3)
C12—C11—C10—C9	-178.84 (19)	N1—C8—C9—C10	-15.0 (3)
C12—C11—C10—S1	0.4 (2)	C7—C8—C9—C10	167.85 (19)
C13—S1—C10—C11	-0.13 (15)	C10—C11—C12—C13	-0.5 (2)
C13—S1—C10—C9	179.21 (15)	C11—C12—C13—S1	0.4 (2)
C2—C1—C6—C5	0.8 (3)	C10—S1—C13—C12	-0.14 (16)
C7—C1—C6—C5	173.47 (17)		

Hydrogen-bond geometry (Å, °)

<i>D</i> —H \cdots <i>A</i>	<i>D</i> —H	H \cdots <i>A</i>	<i>D</i> \cdots <i>A</i>	<i>D</i> —H \cdots <i>A</i>
C11—H11 \cdots N1	0.95	2.41	2.950 (2)	116
C2—H2 \cdots O2	0.95	2.42	2.961 (2)	113
C3—H3 \cdots S1 ⁱ	0.95	2.96	3.810 (2)	149
C15—H15A \cdots O2 ⁱⁱ	0.98	2.98	3.828 (3)	146
C15—H15C \cdots N3 ⁱⁱⁱ	0.98	2.73	3.490 (3)	135
C12—H12 \cdots N1 ^{iv}	0.95	2.95	3.768 (2)	145
C13—H13 \cdots O2 ^v	0.95	2.38	3.191 (2)	143
C14—H14C \cdots O1 ^{vi}	0.98	2.67	3.230 (2)	117

Symmetry codes: (i) $x+1, y, z$; (ii) $x+1/2, -y+1/2, z+1/2$; (iii) $-x+2, -y, -z+2$; (iv) $-x, -y, -z+1$; (v) $x-1/2, -y+1/2, z-1/2$; (vi) $-x+3/2, y-1/2, -z+3/2$.